Computer modelling of the cochlea and the cochlear implant: A review

Vinamra Agrawal[1], Carrie Newbold[2]

[1]Mechanical Engineering, Indian Institute of Technology, Kanpur, India, [2]The HEARing CRC, Carlton, Australia
Department of Otolaryngology, University of Melbourne, Carlton, Australia

In the last few decades, cochlear implants have experienced major developments with intensive studies carried out through experimental and computational analysis. With the rapid increase in computational resources available and the development of efficient computational techniques, computer models of the cochlea and the cochlear implant have become more sophisticated. It is now possible to analyze the micromechanics of the cochlea and the transient response of tissue to external stimulation. This study reviews the major developments in cochlear models, summarizes, and categorizes features of models used in different studies and makes recommendations for future development. The paper is classified into four sections detailing features of the cochlear models, electrodes, electrical stimulation, and software used in different studies. The paper highlights unexplored areas in the model design and suggests additions to develop a better computer model.

Keywords: Cochlear implant, Computer modelling, Cochlear model, Electrical stimulation

Introduction

Cochlear implants have proven to be an effective solution when deafness is created by damage to hair cells. Damage to hair cells renders the cochlea unable to convert mechanical vibrations into neural excitations. Fig. 1 shows a photograph of the Nucleus CI24RE cochlear implant. Over the years, studies have been conducted to optimize the cochlear implant electrode array, varying the electrode shape, type of pulse, and location of the arrays in the cochlea to create effective and safe stimulation. These studies include three-dimensional (3D) computer modelling of the cochlea, with consideration of the structural details of the cochlea, modelling neurons and their arrangement, the type and placement of electrode, the stimulating pulse and the tissue interface between the electrodes and the nerve fibers. The models in each study involved different approximations and limitations. As such a review of these models and their limitations was necessary to encourage further optimization.

The cochlea forms an essential part of the inner ear and is responsible for the conversion of acoustic sound waves to electrical signals in the brain. The cochlea is a bony, fluid-filled, spiral-shaped structure that consists of three cavities namely scala tympani (ST), scala vestibuli (SV), and scala media (SM). In humans, the cochlea spirals to two and a half turns with SV joining ST at the apex, known as the helicotrema. Perilymph fluid is present in SV and ST whereas endolymph fluid fills SM. Reissner's membrane separates SM from SV whereas the basilar membrane (BM) separates SM from ST. The organ of Corti (OC) sits on the BM and consists of four rows of hair cells (three rows of outer (OHC) and one row of inner hair cells (IHC)). Spiral ganglion cells (SGC), the first neural elements in the cochlea, are bipolar neurons that link the hair cells to the cochlear nucleus. Fig. 2 shows a cross-sectional view of cochlea.

Correspondence to: Vinamra Agrawal, Mechanical Engineering, Indian Institute of Technology, Kanpur, 128/92, Block 'G', Kidwai Nagar, Kanpur – 208011, India. Email: vinamraagrawal786@gmail.com

Cochlear models

Effect of coiling

Over the years, researchers have developed 3D numerical models to study various features of the cochlea. One of the key issues addressed by Cai *et al.* (2005) was the influence of coiling on the micro-mechanics of the cochlea. In an earlier paper Manoussaki and Chadwick (2000) found coiling in the cochlea reduces fluid flow impedance. It was concluded that the cochlear curvature helps in the detection of low-frequency sounds at the apex of the cochlea, but does not help for the detection of high frequencies sounds at the base. The radius of curvature was found to be the main parameter responsible for the difference in the influence of coiling in the basal and apical regions of the scala. However, there were certain limitations to this model. The perilymph fluid

DOI 10.1179/1754762811Y.0000000015

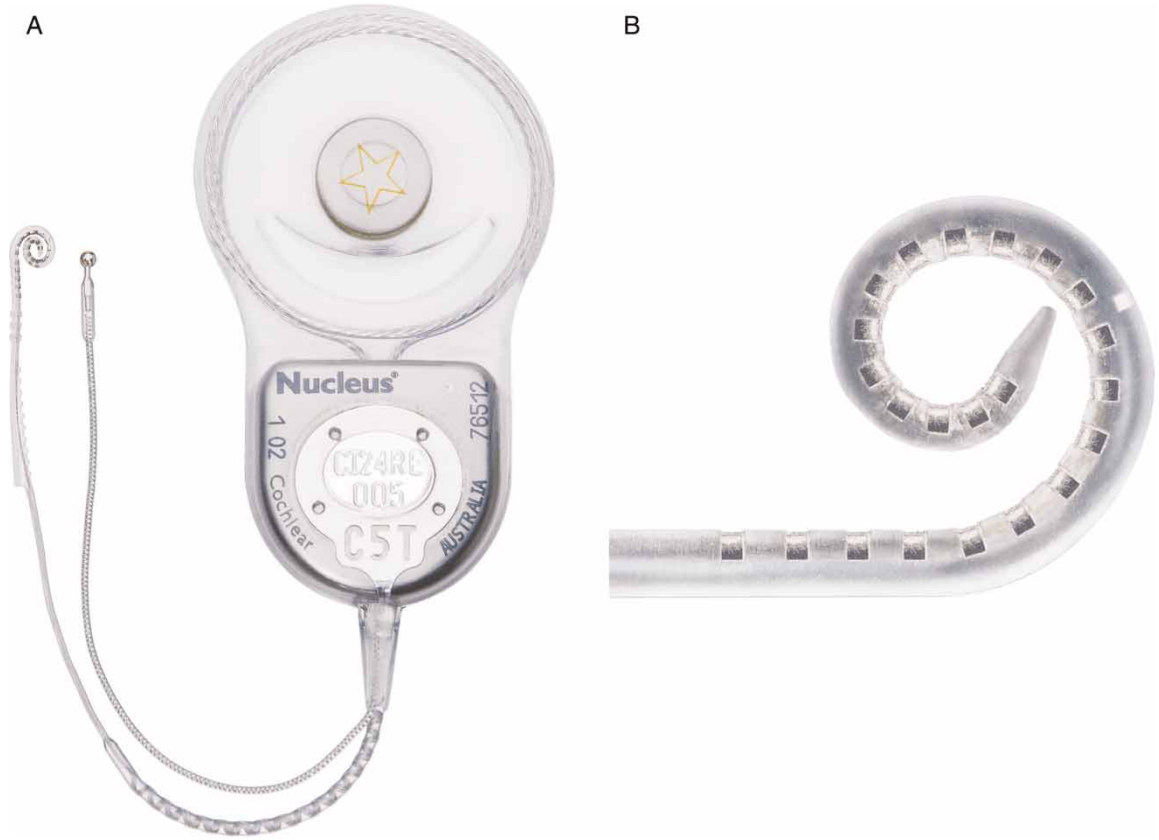

Figure 1 (A) Photograph of the Nucleus CI24RE cochlear implant. (B) Enlargement of the intracochlear electrode array of the Nucleus device (images courtesy of Cochlear Limited 2011).

was approximated as viscous and incompressible (discussed in the following section) and only the relative motions of the cochlear structures were calculated. The study provided a good insight on the significance of coiling in the cochlea. The effect of coiling of the cochlear structure in the presence of the cochlear implant was not studied in Manoussaki *et al.*'s model. However, with the increasing numbers of implantation of patients with residual hearing, the effect of cochlear implant array on sound wave transfer in the perilymph may now be of interest.

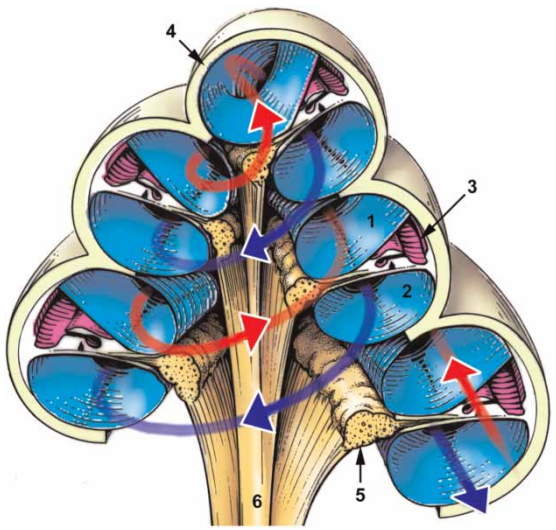

Figure 2 Schematic of the cross section of a cochlea showing direction of fluid flow in the periotic scalae. 1. SM, 2. scala vestibule, 3. ST, 4. spiral ganglion, and 5. auditory nerve. The BM separates the ST from SM. The OC and the hair cells are shown in pink on the BM. (*Source*: drawing by S. Blatrix, from the EDU website http://www.iurc.montp.inserm.fr/cric/audition/english/cochlea/cochlea.htm, by R. Pujol *et al.*, INSERM and University Montpellier).

Fluid and flow properties

Several assumptions regarding the perilymph have been made to study the influence of fluid on sound transmission. Salt and Thalmann (1988) studied the composition of perilymph and endolymph and tabulated their compositions and electrical properties. Böhnke and Wolfgang (1999) created a 3D-finite element model incorporating fluid–structure couplings to study wave propagation and acoustic input impedance of the cochlea. Fluid couplings between the perilymph and stapes footplate, and the round window membrane and elastic cochlear partition were considered. The fluid was assumed to be inviscous and compressible in order to cover fast acoustic waves in the fluid. Cai *et al.* (2005) considered fluid to be viscous and incompressible. The compressibility of the perilymph is negligible for small frequencies, and its influence remains small for high frequencies ($\sim 10^4$ Hz) (Viergever and Kalker, 1974). Viergever and Kalker (1974) also showed the non-linearities

induced in a cochlear model due to the viscosity of the perilymph fluid are negligible.

Mode of model creation

Different studies have used different methodologies to reconstruct their 3D model. Böhnke and Wolfgang (1999) used micro-tomography to obtain 3D images of the scalae. However, they neglected micro-mechanical elements such as hair cells and the OC. Hanekom (2001) created a two-dimensional (2D) cross-section of the cochlea using finite element software. This 2D structure was then extruded into 3D around the central axis of the modiolus. The cross-section was not tapered, however the error induced by this simplification was considered negligible. Rattay *et al*. (2001) also created a simplified model of the cochlea from a single cross-section. First they created a rotationally symmetric model by using a large number of nodes, and then these key points or nodes were reduced to create a simplified 3D model. Another approach mentioned by Rattay *et al*. (2001) and used by Briaire and Frijns (2000) was to use 20 μm histological sections of the cochlea and to reconstruct a 3D model similar to that of a real cochlea. Lim *et al*. (2005) extracted a contour from the standard section of human cochlea and used a helico-spiral approximation introduced by Yoo *et al*. (2000) for calculating the curvature of the cochlea. The mode of development chosen depended on the objective of the study for example, Rattay *et al*. (2001) focused on modelling the neuron arrangement rather than the intricacies of the scalae and as such, a simplified model of the cochlea was sufficient.

Level of anatomical detail

One clear difference in the published models is the level of anatomical detail required for each study. Böhnke and Wolfgang (1999) modelled the dimensional aspect of scala but neglected the details of the micro-mechanical elements as their analysis focused on wave propagation and input impedance of the cochlea. Alternatively, Kolston and Ashmore (1996) modelled the BM with the IHCs and OHCs to study the dynamics of the BM, OC, and hair cells while transferring sound waves. Frijns *et al*. (1995) compared a rotationally symmetric model and a spiral model of the cochlea coupled with an active nerve fiber model to analyze potential distributions and neural excitation patterns of electrically stimulated cochlea. Briaire and Frijns (2000) introduced tapering of the scala in their model. The field patterns of rotationally symmetric and spiral nerve fiber arrangement were computed. In a later paper, Briaire and Frijns (2006) improved the nerve fiber model, by using an unmyelinated cell body and an unmyelinated pre-somatic region. This nerve fiber model was considered to be much a better approximation of the human nerve fiber than the generalized Schwartz–Eikhof–Frijns (GSEF) model used previously. Like the mode of creation, the level of anatomical detail required also depended on the intended use of the model (further details in neural elements section).

Mechanical properties

The material properties of each component of the cochlea have to be assigned to allow for mechanical analysis. Lim *et al*. (2005) used a Poisson's ratio of 0.3 for the cochlear components. Two zones of the BM were created and different elastic moduli were assigned to each (Table 1). Böhnke and Wolfgang (1999) used two different values of Young's modulus of the cochlea partition for the transverse and longitudinal direction (Table 1). Kolston and Ashmore (1996) studied the dynamics of the BM, OC, and hair cells and used coupling impedance values BM, OHC, Deiters' cells, tectorial membrane, and reticular lamina for their calculation. These coupling impedance values consisted of a stiffness component and a resistive component (Table 1). Cai *et al*. (2005) used the mechanical properties from their earlier model (Cai *et al*., 2004) which are listed in Table 1.

Electrical properties

The conductivity data of various cochlear components used by Briaire and Frijns (2000), Hanekom (2001), Rattay *et al*. (2001), and Frijns *et al*. (1996) were adapted from Finley *et al*. (1990) and scaled appropriately. In all cases, the cochlear components were assumed to be completely resistive to simplify the calculations. Frijns *et al*. (1995) used boundary element method (BEM) for their calculations. While BEM can handle capacitive effects, neglecting capacitance allowed evaluation of time-varying stimuli without considering charge storage effects. Spelman *et al*. (1982) showed that the impedance inside and outside the scalae were mostly resistive for frequencies between 8 Hz and 12.5 kHz. Using this, Hanekom (2001) considered the cochlear tissues as pure resistances up to the first approximation. However, a detailed analysis including capacitive properties of the cochlear components could also be performed (further details in the electrode–tissue interface section).

Neural elements

In order to study the method of transfer of electric stimulus through the nerve fibers in the cochlea, Frijns *et al*. (1995) compared the neural response in a rotationally symmetric and spiral arrangement of nerve fibers. A GSEF model of the nerve fiber, based on a mammalian nerve fiber was defined

Table 1 Material properties used in computer models of the cochlear tissue and electrode array

Element		Reference	Elastic modulus (MPa)	Stiffness (MN/m^3)	Resistance ($MN\ s/m^3$)
Pt/Ir/PTFE		a	8270	–	–
Silicone elastomer		a	0.45	–	–
Compact bone		a	20 000	–	–
Stapes footplate		b	12 000	–	–
Keratin		a	3000	–	–
Annular ligament		b	0.7	–	–
Round window membrane		b	9.8	–	–
BM	Overall	c	–	300 000	0.17
	Apex	d	200	–	–
	Base	d	30	–	–
	Transverse direction	b	100	–	–
	Longitudinal direction	b	0.01	–	–
	Fibers	b	1900	–	–
	Ground substance	b	0.2	–	–
Tectorial membrane	Apex	d	0.001	–	–
	Base	d	0.004	–	–
	Vertical sulcus side	c	–	30 000	0.017
	Vertical strial side	c	–	30 000	0.017
	Horizontal sulcus side	c	–	60 000	0.017
	Horizontal strial side	c	–	300 000	0.17
OC	Apex	d	0.0002	–	–
	Base	d	0.002	–	–
Hensen cells	Apex	d	0.001	–	–
	Base		0.005	–	–
Reticular lamina	Apex	d	0.03	–	–
	Base	d	0.5	–	–
	Vertical	c	–	300 000	0.17
	Horizontal	c	–	3 000 000	1.7
	Vertically to tectorial membrane	c	–	3 000 000	1.7
Pillar cells	Apex	d	0.05	–	–
	Base	d	0.8	–	–
	Vertical	c	–	3 000 000	1.7
	Horizontal	c	–	300 000	0.17
	Tilting	c	–	3 000 000	1.7
Deiters' cells	Overall	c	–	30 000	0.017
	Apex	d	0.01	–	–
	Base	d	0.1	–	–
Outer hair cells	Overall	c	–	3	0.0017
	Apex	d	0.006	–	–
	Base	d	0.009	–	–
Inner hair cells	Apex	d	0.004	–	–
	Base	d	0.007	–	–

a: Lim *et al.* (2005); b: Böhnke and Wolfgang (1999); c: Kolston and Ashmore (1996); d: Cai *et al.* (2004).

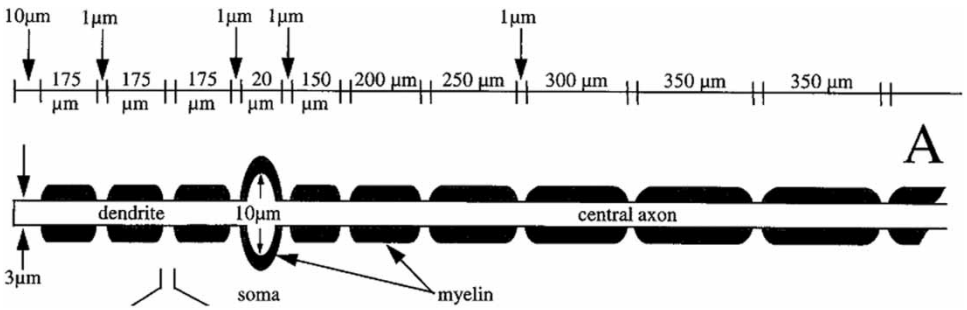

Figure 3 GSEF model used by Frijns *et al*. (1995) (reprinted with permission from Elsevier).

(Fig. 3). The nerve fiber model consists of 15 myelinated segments and 16 unmyelinated nodes. This model was also used in Hanekom (2001) and Briaire and Frijns (2000). Hanekom (2001) used a finite element cochlear model containing 90 segments, creating 91 potential values and as such 91 nerve fibers were used. To study the response of degenerated nerve fibers, Hanekom (2001) also performed simulations using a truncated GSEF model. Briaire and Frijns (2000) compared the potential distributions of a rotationally symmetric model and a spiral-shaped nerve model. In their later work, Briaire and Frijns (2006) improved the GSEF model for a better representation of human nerve fiber model.

Animal model variations

Another noticeable point is the difference between human and animal cochlea used in the studies. Hatsushika *et al*. (1990) conducted experiments to obtain dimensions of human and cat cochlea and observed a few noticeable structural differences between them. Briaire and Frijns (2000) also noted the structural difference between guinea pig and human cochlea but found its influence on excitation patterns negligible for intracochlear electrodes. Shera *et al*. (2001) computed a dimensionless measure of 'sharpness' or frequency selectivity of tuning, a dimensionless measure of group delays of stimulus frequency otoacoustic emissions of BM and a relating factor of human, cat, and guinea pig cochlea. While the authors noted the structural difference between human, cat, and guinea pig cochleae a little interspecies variation was found in the computed quantities.

Electrodes

Material and mechanical properties

The cochlear implant electrode array is commonly made of platinum (Pt; 90%) – iridium (Ir; 10%) wires coated with polytetrafluoroethylene (PTFE) or another insulative material, connecting to Pt electrodes within a silicone elastomer carrier. The elastic moduli and Poisson's ratio of the electrode array used in Lim *et al*. (2005) are presented in Table 1. The stiffness of the electrode array varies inside the cochlea depending upon the arrangement of wires. The overall stiffness of the electrode array must be kept to a minimum to allow it to easily bend around the modiolus of the cochlea (Lim *et al*., 2005).

Electrode geometry

Hanekom (2001) modelled electrode shape as banded and point and compared their influence on potential distributions and nerve excitation patterns. The potential maxima and minima at the nerve fiber terminals differed substantially between banded and point electrode geometry for the same stimulus. When electrodes were closer to fiber terminals, point electrode arrays produced excitation patterns similar to those produced by arrays close to the nerve fibers, whereas banded electrode arrays produced excitation patterns similar to those produced by arrays far from the target nerve fibers. Banded electrode geometry also helped to limit excitation spread when the electrode array was placed on the outer wall of ST. The use of point electrodes was recommended if the precise location of the electrodes can be controlled and monitored. Alternatively, banded geometry can provide lower threshold values if the exact location cannot be controlled.

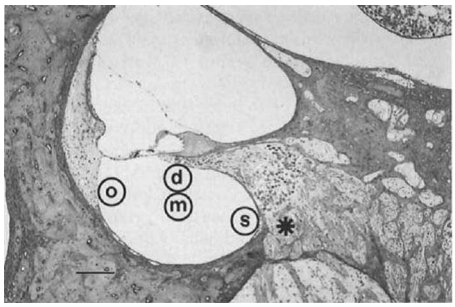

Figure 4 Location of placement of electrodes in basal turn of cat cochlea. Asterisk denotes location of Rosenthal's canal in human cochlea (reprinted from Shepherd *et al*. (1993) with permission from Elsevier).

Electrode location

The effects of the electrode position on neural excitation were first studied by Shepherd *et al*. (1993) on an animal model of the auditory nerve of 10 healthy adult cats. The electrodes were inserted in four different locations (Fig. 4): outer wall of ST (O), middle of ST (M), adjacent to the modiolus close to SGC (S), and underneath peripheral dendrites (D). It was found that the excitation threshold dropped by 10 dB as electrodes were moved from O to D. A reduction in the rate of growth of waveform amplitude with stimulus current was also observed as electrodes were moved from O to D. From the basis of their findings, it was suggested the location S is optimum for neural stimulation with least damage to auditory nerve.

Hanekom (2001) modelled, through a computer model, two array locations for banded geometry electrodes: medial position close to the modiolus and lateral position close to the outer wall of ST. For point electrodes, three positions were considered: medial position close to modiolus, central position, and lateral position close to outer wall of ST. It was shown that the arrays in the lateral position, being closer to the nerve fiber terminal, caused potential maxima and minima at the nerve fiber terminals. In the case of degenerated nerve fibers, an increase in excitation threshold was observed for lateral array locations, while excitation threshold decreased for medial locations. Like Shepherd *et al*. (1993), it was recommended to place the electrodes closer to the modiolus. For electrodes placed toward the outer wall of ST, lower thresholds were predicted for nerve fibers close to the basal electrode than for nerve fibers close to the apical electrode. A greater excitation spread was also shown when the array was placed far from the modiolus. Electrode positions nearer to the modiolus caused only localized excitation spread.

Ho *et al*. (2004) proposed a new method of placing the return electrode, normally implanted extracochlearly. It was shown that the modiolar current can be increased three times if a return electrode is

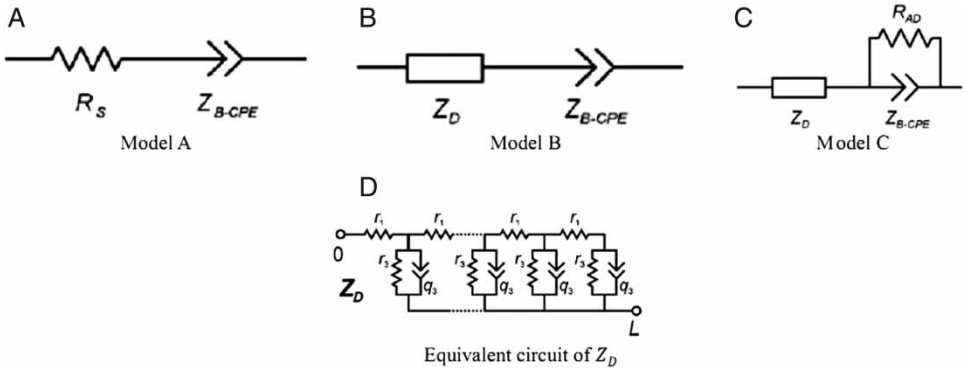

Figure 5 (A) Model A, (B) Model B, (C) Model C, and (D) equivalent circuit of Z_D used by Duan *et al.* (2004) (reprinted with permission from Elsevier).

placed in the modiolus. However, certain surgical complications can arise while inserting the electrode in the modiolus. There is a possibility of leakage of cerebrospinal fluid during surgery while drilling a hole in the modiolar wall. There is also a huge risk of damage to auditory nerve during drilling. There are problems of ectopic stimulation, but some potential solutions to this problem were suggested.

Modelling electrode–tissue interface

The electrode–tissue interface undergoes constant changes soon after cochlear implantation due to inflammation and bone growth. Clinically, only the maximum or total electrode impedance of the electrode–tissue interface can be determined. Thus computer and animal models are required to determine the resistive and capacitive changes that occur to the interface following implantation and electrical stimulation. Many experimental studies have been conducted to monitor the changes in the impedance over different periods of time. Duan *et al.* (2004) proposed three electrical equivalent circuits (Fig. 5) to model the electrode–tissue interface over different periods of time. Model A (Fig. 5A), used to study the impedance data soon after surgery includes a resistive component R_S for electrolyte resistances in series with a constant phase boundary impedance Z_{CPE}. Diffusive impedance Z_D (Fig. 5D) replaces R_S in Model B (Fig. 5B) to account for the charge transport at the living biological electrolyte adjacent to the electrodes. An adsorption resistance R_{AD} was added in parallel to the boundary impedance Z_{CPE} in Model C (Fig. 5C) to account for the adsorption at the electrodes. It was shown that the effect of R_{AD} is only significant in frequencies less than 0.1 Hz.

Troy *et al.* (2006) developed a computer model to study the effects of electrode–electrolyte interface on electric potential and current density surrounding metal microelectrodes using thin layer approximation. It was shown that at low potentials the electrode–electrolyte interface has a substantial effect, but as the potential is raised, the effect of interface becomes negligible. McAdams and Jossinet (1994) theoretically studied the onset of non-linearity in the impedance of electrode–electrolyte interface. It was shown that the charge transfer resistance was the source of the observed non-linear behavior.

Choi *et al.* (2006) demonstrated the significance of the electrode–tissue interface though a computational study. Three models of a cochlea, circular with half turns, circular with one turn, and spiral with one turn, were studied. Impedance matrix using monopolar stimulation was computed and compared with experimental observations. Tapering of the cochlea and equivalent model of electrode–tissue interface were introduced and changes in impedance matrix were noted. It was observed that the addition of tapering and the electrode–tissue interface to the model improved its resemblance to actual cochleae.

Lai and Choi (2007) also studied effects of the electrode–tissue interface on stimulation response and impedance. A new idea of replacing equivalent circuit of electrode–tissue interface by a thin film was introduced and studied. A 0.5 mm thick layer with complex permittivity was used in this study. The complex permittivity was based on faradic resistance and capacitance calculated using Ohm's Law. Voltage and impedance values of three models were studied: without any interfacial layer, using electrical equivalent of the interface and using a thin film layer. Although results of the thin film and the electrical equivalent model were the same, it was argued that since thin film removes the circuit from the picture, it provides more flexibility to the model.

Electrical stimulation

To provide the cochlear implant with suitable excitation, different aspects of electrical stimulation have been explored. The focal point of such studies has been the stimulation mode, or choice of electrode pair. While modelling different electrode configurations is necessary for impedance and power optimizations, other aspects of electrical stimulation like electrical stimulus and pulse shapes are yet to be

studied in a computational model. A few experimental studies have been done to study effects of different pulse shapes on auditory responses, but these are mostly limited to animal cochlea.

Stimulation mode

Hanekom (2001) studied six different electrode configurations: narrow bipolar (NBP), bipolar (BP), bipolar + 1 (BP + 1), bipolar + 2 (BP + 2), bipolar + 3 (BP + 3), and apical reference (AR) configuration. It was shown that BP, BP + 1; BP + 2, and BP + 3 had little effect on spread of excitation which confirmed findings of Shepherd *et al*. (1993). The use of wide configurations up to BP + 3 was shown to be safe if the threshold could not be achieved by narrow spaced configuration. Electrode separation alone cannot limit excitation spread to a large extent. However, the electrode separation can be used for a fine adjustment on spread of excitation. AR configuration was shown to localize excitation when nerve fibers were very close to modiolus. Laydrus (2007) compared monopolar and bipolar electrode configuration and obtained remarkably localized stimulation pattern in bipolar stimulation. Current density around stimulation area in bipolar electrode configuration was found to be smaller than monopolar electrode configuration.

Electrical stimulus

The impedance of the electrode–tissue interface undergoes constant changes after implantation. Electrical stimulation also contributes to these changes (Newbold *et al*., 2004). In order to prevent injection of any residual charges, charge-balanced biphasic (BP) pulses are commonly used. Monophasic stimulation or any DC current can lead to neural damage because it induces irreversible reactions such as electrode dissolution and electrolysis of water. However, in an experimental study, Miller *et al*. (2001) proved that monophasic pulses have lower threshold values and hence are more efficient. The pulse parameters, current, pulse width and rate, are used to define the electrical stimulus used in cochlear implants. A pulse with a current magnitude between 100 and 1000 μA and pulse width ranging from 25 to 100 μs was used by Laydrus (2007). Hanekom (2001) used 200 μA DC stimulation current to calculate equipotential lines. Ho *et al*. (2004) used alternating current stimulus of 100 Hz with amplitude of 100 μA in their study. A 200 μs/phase biphasic pulse was used to study excitation profiles by Frijns *et al*. (1995).

Pulse parameters

Many different experimental studies have been conducted on animals and humans to study optimal pulse parameters (shape, rate, and width), for safe stimulation and clinical use. Studies conducted by Macherey *et al*. (2006) focused on pseudo-monophasic (PS) and delayed pseudo-monophasic (DPS) pulses and compared them to BP stimulation. The effect of pulse shape on safety of stimulation was studied and it was found that PS-cathode first and DPS-cathode first increase safe charge injection limit than BP pulse. However, the polarity of the leading phase did not affect thresholds of PS and DPS. Further, it was found that alternating monophasic with 40 ms interpulse gap (IPG) resists nerve fatigue better than BP pulse with an 800 μs IPG.

Miller *et al*. (2001) also conducted experimental analysis to study auditory nerve responses to monophasic, PS, and biphasic stimulation. While this topic is extensively researched experimentally, a comprehensive computational study could be done analyzing pulse parameters of stimulation on a 3D computer generated model.

Software

Most of the studies used ANSYS software for finite element analysis or boundary element analysis, like Lim *et al*. (2005), Böhnke and Wolfgang (1999), Rattay *et al*. (2001), and Laydrus (2007). For model construction involving the reconstruction of histological section images, Wang *et al*. (2006) used AMIRA software. However, in-house software was developed for 3D surface rendering and visualization (Wang *et al*., 2006). Yoo *et al*. (2000) used analyze image analysis and a visualization software package for the segmentation of cochlear canal from round window. Lim *et al*. (2005) used Rapidia software for the reconstruction of CT scanned images.

Discussion

Different cochlear models with varying anatomical details have been employed depending upon the focus of the study. An overall table (Table 2) summarizing and comparing cochlear models is presented at the end of the paper. The influence of coiling of cochlea on sound propagation and frequency selection has been studied extensively and many studies have incorporated coiling in their model. The use of coiling is recommended when the issue under analysis is significantly influenced by the coiling such as study of flow impedance. Evaluation of possible non-linearities in the model must be done and if the error induced by the coiled behavior is significant compared to other factors then a spiralling structure should be used. The tapering of the scalae was neglected while analyzing auditory nerve responses by Rattay *et al*. (2001) and Briaire and Frijns (2000). On the contrary, tapering of the scalae was employed by Lim *et al*. (2005) to study the mechanical effects of electrode insertion. Thus, the level of anatomical details incorporated in the model was governed by the primary focus of the

Table 2 An overall table summarizing mechanical models, electrodesm and electrical stimulation used in different studies

	Material	Electrode geometry	Electrode location	Electrode configuration	Electrical stimulus	Pulse parameters
Electrodes and electrical stimulation						
Frijns *et al.* (1995)	N/A	Point	Longitudinally along BM	Bipolar	Biphasic	Time period – 200 μs per phase
Kolston and Ashmore (1996)	Electrode and electrical stimulation not studied in this paper					
Böhnke and Wolfgang (1999)	Electrode and electrical stimulation not studied in this paper					
Briaire and Frijns (2000)	N/A	Point	Center of scala tympani	Both monopolar and bipolar were used	N/A	1 mA current
Hanekom (2001)	N/A	Banded and point	Medial position close to modiolus – banded and point Lateral position close to outer wall – banded and point Central position – point geometry	6 electrode configurations	DC	Magnitude 200 μA
Rattay *et al.* (2001)	N/A	Point electrodes	Center of scala tympani	Monopolar, bipolar and quadrupolar	Monophasic and biphasic	100 μs pulses
Cai *et al.* (2005)	Electrode and electrical stimulation not studied in this paper					
Lim *et al.* (2005)	Properties listed in Table 1	16 metal wires Diameter 0.6 mm at tip Diameter 0.8 mm at base 20 mm length of wire	Electrical stimulation not studied in this paper			
Briaire and Frijns (2006)	N/A	Electrode array	Electrode array inserted throughout the cochlea	N/A	Biphasic cathodic first	37.5 μs/phase
Laydrus (2007)	Same as ST or scar tissue depends upon simulation	Octagonal with a carrier core, conductor layer and four external layers	Medial position close to modiolus Lateral position close to outer wall	22 electrodes with 0.5 mm length Interelectrode spacing 0.5 mm	Biphasic	Magnitude – 100–1000 μA Time period – 25–100 μs

	Coiling	Fluid and flow properties	Mode of model creation	Level of anatomical details	Mechanical properties	Electrical properties	Neural elements
Mechanical models							
Frijns (1995)			Cochlear model not designed in this paper				
Kolston and Ashmore (1996)	No	N/A	Micromechanical modelling of OC components	Tectorial membrane, OC, RM Deiter's cells, pillars of Corti reticular lamina, OHC, IHC	Listed in Table 1	N/A	N/A
Böhnke and Wolfgang (1999)	Yes	Linear, inviscous, compressible	Spline interpolation of microtomographical images	2 scalae, dimensional aspects No micromechanical elements	Listed in Table 1	N/A	N/A
Briaire and Frijns (2000)	Yes	N/A	Interpolation of 20 μm histological sections	Coiled tapered structure 3 scalae, OC, spiral ligament OC, Reissner's membrane	N/A	Resistive values Values scale according to size	GSEF model 2 types of arrangement Spiral, rotationally symmetric Nerve model
Hanekom (2001)	Yes	N/A	Extrusion of 2D cross section around central axis	No tapering of cross section Effects of conduction through fluid Axon layer was modelled Cylindrical boundary of entire model	N/A	Resistive values used from Finley *et al.* (1990)	Truncated GSEF model 91 nerve fibers
Rattay *et al.* (2001)	Yes	N/A	Extrusion from a single cross-sectional image	Approximated structure: Reissner's membrane, OC 1.5 turns modelled	N/A	Resistive values	Short and long types of neurons Long neuron – standard neuron Short neuron - 3 nodes of Ranvier
Cai *et al.* (2005)	Yes	Viscous, incompressible	N/A	Coiling Cellular structure within OC interaction with CP and fluid	BM : clamped annular plate OC and TM : Voigt solids Listed in Table 1	N/A	N/A
Lim *et al.* (2005)	Yes	N/A	Interpolation of contour using helico-spiral approx.	Coiled tapered structure 3 scalae BM divided into pectinate and arcuate	Listed in Table 1	N/A	N/A
Briaire and Frijns (2006)	Yes	N/A	Same as Briaire and Frijns (2000)	Same as Briaire and Frijns (2000)	N/A	Same as Briaire and Frijns (2000)	Improved GSEF model
Laydrus (2007)	No	N/A	Linear extrusion of cross section along *z* direction	3 scalae, OC, RM	N/A	Resistive values adopted from Finley *et al.* (1990)	N/A

study and the extent of its influence on the results. The properties of the perilymph fluid varied in different studies. While researchers have shown that the effect of viscosity and compressibility was negligible within operating frequencies, flow properties must be analyzed to arrive at a justified conclusion. Electrical properties of the scalae used in most studies were based on values obtained by Finley *et al*. (1990). These values being purely resistive ignore the charge storage capacity of the cochlear components and hence introduce an additional error.

The material of the electrode wire is a standard alloy, however new materials are constantly being researched. The selection of electrode geometry affects the threshold of excitation and excitation spread (and accuracy of placement of electrodes). Manufacturing constraints also govern feasibility of electrode geometry selection; point electrodes are difficult to manufacture. The placement of electrode also controls the threshold value and excitation spread. Placement close to the modiolus is recommended for lower threshold values. Modelling the electrode–tissue interface is still one of the less explored areas of the cochlear implants. Analysis of the electrode–tissue interface is necessary for monitoring power requirements of the implants and so a generalized equivalent electrical circuit must be incorporated in the cochlear model to get a better understanding of impedance changes over time and frequency. Many experimental studies have been conducted to study the possibility of safe stimulation and lower thresholds by varying the pulse parameters. However, a computational study for the same is needed to be incorporated in main model.

This study goes through the major features in cochlear model development by comparing different studies. Issues like fluid-flow properties, modelling of electrode–tissue interface, and inclusion of capacitive properties in the cochlear models are still unresolved. The study gives researchers a better view of what has previously been done and which areas still remain unexplored. Several suggestions have been made throughout the paper to increase sophistication of future models.

Acknowledgments

The authors thank the international exchange program Summer Undergraduate Research Grant for Excellence (SURGE) organized by Indian Institute of Technology Kanpur and hosted by University of Melbourne. The authors acknowledge the financial support of the HEARing CRC, established and supported under the Australian Government's Cooperative Research Centres Program.

References

Böhnke F., Wolfgang A. 1999. Three dimensional finite element model of the human cochlea including fluid–structure couplings. *Journal for Oto-Rhino-Laryngology and its Related Specialities*, 61: 305–310.

Briaire J.J., Frijns J.M. 2000. Field patterns in a 3D tapered spiral model of the electrically stimulated cochlea. *Hearing Research*, 148(1–2): 18–30.

Briaire J.J., Frijns J.H. 2006. The consequences of neural degeneration regarding optimal cochlear implant position in scala tympani: a model approach. *Hearing Research*, 214: 17–27.

Cai H., Manoussaki D., Chadwick R. 2005. Effects of coiling on the micromechanics of the mammalian cochlea. *Journal of the Royal Society Interface*, 2: 341–348.

Cai H., Shoelson B., Chadwick R.S. 2004. Evidence of tectorial membrane radial motion in a propagating mode of a complex cochlear model. *Proceedings of the National Academy of Sciences of the United States of America*, 101(16): 6243–6348.

Choi C.T.M., Lai W., Lee S. 2006. A novel approach to compute the impedance matrix of a cochlear implants system incorporating an electrode-tissue interface based on finite element method. *IEEE Transactions on Magnetics*, 42(4): 1375–1378.

Duan Y.Y., Clark G.M., Cowan R.S. 2004. A study of intra-cochlear electrodes and tissue interface by electrochemical impedance methods in vivo. *Biomaterials*, 25(17): 3813–3828.

Finley C.C., Wilson B.S., White M.W. 1990. Models of neural responsiveness to electrical stimulation. In: Miller JM, Spelman FA (eds.), Cochlear implants. New York: Springer, Verlag, p. 55–96.

Frijns J.H., de Snoo S.L., Schoonhoven R. 1995. Potential distributions and neural excitation in a rotationally symmetric model of the electrically stimulated cochlea. *Hearing Research*, 87: 170–86.

Frijns J.H., de Snoo S.L., ten Kate J.H. 1996. Spatial selectivity in a rotationally symmetric model of the electrically stimulated cochlea. *Hearing Research*, 95: 33–48.

Hanekom T. 2001. Three-dimensional spiralling finite element model of the electrically stimulated cochlea. *Ear and Hearing*, 22(4): 300–315.

Hatsushika S., Shepherd R.K., Tong Y.C., Clark G.M., Funasaka S. 1990. Dimensions of the scala tympani in the human and cat with reference to cochlear implants. *Annals of Otology, Rhinology and Laryngology*, 99: 871–876.

Ho S.Y., Wiet R.J., Ritcher C.P. 2004. Modifying cochlear implant design: advantages of placing a return electrode in the modiolus. *Otology and Neurotology*, 25(4): 497–503.

Kolston P.J., Ashmore J.F. 1996. Finite element micromechanical modelling of the cochlea in three dimensions. *The Journal of the Acoustical Society of America*, 99(1): 455–67.

Lai W., Choi C.T.M. 2007. Incorporating electrode-tissue interface to cochlear implants models. *IEEE Transactions on Magnetics*, 43(4): 1721–1724.

Laydrus N. 2007. Modelling the current spread in human cochlea through electrode geometries of a cochlear implant. Thesis, University of New South Wales.

Lim Y.S., Park S.I., Kim Y.H., Oh S.H., Kim S.J. 2005. Three-dimensional analysis of electrode behaviour in a human cochlear model. *Medical Engineering and Physics*, 27(8): 695–703.

Macherey O., Wieringen A.V., Carlyon R.P., Deeks J.M., Wouters J. 2006. Asymmetric pulses in cochlear implants: effect of pulse shape, polarity and rate. *Journal of the Association in Research in Otolaryngology*, 7: 253–266.

Manoussaki D., Chadwick R. 2000. Effects of geometry on fluid loading in a coiled cochlea. *SIAM Journal on Applied Mathematics*, 61(2): 369–386.

McAdams E.T., Jossinet J. 1994. The detection of the onset of electrode–electrolyte interface impedance nonlinearity: a theoretical study. *IEEE Transactions on Biomedical Engineering*, 41(5): 498–500.

Miller C.A., Robinson B.K., Rubinstein J.T., Abbas P.J., Runge-Samuel C.L. 2001. Auditory nerve responses to monophasic and biphasic electrical stimuli. *Hearing Research*, 151: 79–94.

Newbold C., Richardson R., Huang C.Q., Milojevic D., Cowan R.S., Shepherd R.K. 2004. An in vitro model for investigation impedance changes with cell growth and electrical stimulation: implications for cochlear implants. *Journal of Neural Engineering*, 1(4): 218–227.

Rattay F., Leao R.N., Fedlix H. 2001. A model of the electrically excited human cochlear neuron. II. Influence of the three-dimensional cochlear structure on neural excitability. *Hearing Research*, 153: 64–79.

Salt A.N., Thalmann R. 1988. Cochlear fluid dynamics. In: Jahn AF, Santos-Sacchi JR (eds.), Physiology of the ear. New York: Raven Press, p. 341–357.

Shepherd R.K., Hatsushika S., Clark G.M. 1993. Electrical stimulation of the auditory nerve: the effect of electrode position on neural excitation. *Hearing Research*, 66: 108–120.

Shera C.A., Gulnan Jr. J.J., Oxenham A.J. 2001. Revised estimated of human cochlear tuning from otoacoustic and behavioural measurements. *Proceedings of the National Academy of Sciences of the United States of America*, 99(5): 3318–3323.

Spelman F.A., Clopton B.M., Pfingst B.E. 1982. Tissue impedance and current flow in the implanted ear: implications for the cochlear prosthesis. *Annals of Otology, Rhinology and Laryngology*, 98: 3–8.

Troy J.B., Cantrell D.R., Taflove A., Ruoff R.S. 2006. Modelling the electrode–electrolyte interface for recording and stimulation electrodes. *Annual International Conference of the IEEE Engineering in Medicine and Biology Society*, 1: 879–81.

Viergever M.A., Kalker J.J. 1974. Localization of non-linearities in the cochlea. *Journal of Engineering Mathematics*, 9(1): 11–20.

Wang H., Northrop C., Burgess B., Liberman M.C., Merchant S.N. 2006. Three dimensional virtual model of the human temporal bone: a stand-alone, downloadable teaching tool. *Otology and Neurotology*, 27(4): 452–7.

Yoo S.K., Wang G., Rubinstein J.T., Vannier M.W. 2000. Three-dimensional geometric modelling of the cochlea using helico-spiral approximation. *IEEE Transactions on Biomedical Engineering*, 47(10): 1392–1402.